DOI: 10.15201/hungeobull.71.3.1 Hungarian Geographical Bulletin **71** 2022 (3) 213–229.

The relationship between ignimbrite lithofacies and topography in a foothill setting formed on Miocene pyroclastics – a case study from the Bükkalja, Northern Hungary

Tamás BIRÓ[1], Mátyás HENCZ[1], Tamás TELBISZ[1], Zoltán CSERI[1] and Dávid KARÁTSON[1]

Abstract

Units with extremely variable erodibility are typical in the succession of pyroclastic-dominated volcanic fields. Welded ignimbrites are usually resistant to erosion, thus, they often appear as positive landforms, i.e., mesas or tilted plateaus after millions of years of denudation. The Bükkalja Volcanic Area being part of the most extended foothill area of the North Hungarian Mountains, is composed predominantly of Miocene ignimbrites, where the frequency distributions of elevation a.s.l., slope, aspect, as well as topographic openness, were investigated using a 30 m resolution SRTM-based digital surface model at four sample areas located at different relative distances from the assumed source localities of the ignimbrites, showing both non-welded and welded facies. The degree of dissection was also examined along swath profiles. The topography of the sample area closest to the source localities is dominated by slabs of moderately dissected welded ignimbrites, gently dipping towards SE. Farther away from the source the topography is dominated by erosional valleys and ridges, resulting in a narrower typical elevation range, a higher proportion of pixels with greater than 5° slope, higher frequencies of NE and SW exposures, and more significant incision resulted in more frequent pixels with positive topographic openness less than 1.5 radians here. Higher thicknesses and emplacement temperatures of ignimbrites, often showing welded facies are more common closer to the source vent. Thus, the erosional pattern around calderas can be used to draw conclusions on the spatial extent of the most intense ignimbrite accumulation, i.e., the location of eruption centres even in highly eroded ignimbrite fields.

Keywords: Bükkalja, ignimbrite, Miocene, welded ignimbrite, SRTM, swath analysis, topographic openness, digital elevation model, differential erosion

Received July 2022, accepted August 2022.

Introduction

Pyroclastic successions developed around caldera clusters often host units showing contrasting resistance to erosion. Welded ignimbrites are usually characterized by extremely low erodibility, often forming plateaus existing for millions of years, sometimes as inverted relief (Adams, B.A. and Cooper, F.J. 2020; Van Wyk de Vries, B. *et al*. 2022). Tilted ignimbrite plateaus exceeding $10^{4\text{-}5}$ km^2 lateral extent dissected by canyons at their edges due to fluvial erosion are well-known landforms of many ignimbrite fields around the Earth: among others at the western edge of the Central Andes (Székely, B. *et al.* 2014), at the Taupo Volcanic Zone at the North Island of New Zealand (Leonard, G.S. *et al.* 2010) or around many calderas in the United States (e.g., the Pajarito Plateau at the eastern flank of the Valles Caldera; Crowe, B.M. *et al.* 1978). The Bükkalja study area presented in this paper does not belong to the largest ignimbrite fields in a global comparison, but its in-depth volcanological research and the long-term erosion since Mi-

[1] Department of Physical Geography, Institute of Geography and Earth Sciences, ELTE Eötvös Loránd University. Pázmány Péter sétány 1/C, H-1117, Budapest, Hungary. Corresponding author's e-mail: tamas.biro@ttk.elte.hu

ocene times makes it a perfect study area that can provide valuable results for analysing the geomorphological evolution of ancient, deeply eroded ignimbrite fields hosting plateaus of welded ignimbrites.

The Bükkalja is the most extended foothill of the North Hungarian Mountains, forming a gradually descending (from 400 to 130 m a.s.l.) hilly region between the Mesozoic carbonate block of the Bükk Mountains and the Quaternary fluvial sediments of the Great Hungarian Plain (*Figure 1*, Dobos, A. 2002; Hevesi, A. 2002). The Bükkalja exposes the thickest (often exceeding 500 m) and most complex succession of silicic pyroclastics of Miocene age in the northern part of the Pannonian Basin (Szakács, A. *et al.* 1998; Lukács, R. *et al.* 2018, 2022). Moreover, the surface occurrence of the Miocene pyroclastics at the Bükkalja is the largest in Northern Hungary, covering an area of about 10 x 40 km (Less, Gy. *et al.* 2005). Consequently, the Bükkalja has been the focus of both volcanological and geomorphological studies in recent decades: Volcanological research has explored the stratigraphic units of the Bükkalja pyroclastic succession, the character of the volcanism, as well as the spatial dimensions and age of individual eruptive events (Capaccioni, B. *et al.* 1995; Szakács, A. *et al.* 1998; Lukács, R. *et al.* 2007, 2015, 2018, 2022; Biró, T. *et al.* 2020; Hencz, M. *et al.* 2021a, b; Karátson, D. *et al.* 2022).

Geomorphological studies on the Bükkalja have been carried out in detail to investigate the connection between structural geology, lithology, landscape evolution and landforms, focussing on the following questions: how lithology is related to the drainage network (Vágó, J. 2012; Pecsmány, P. 2021), which lithological conditions enhance the preservation of relict surfaces (Vágó, J. and Hegedűs, A. 2011), how the deep structure revealed by seismic sections is reflected in the course of major fluvial valleys (Pecsmány, P. and Vágó, J. 2020), and where fault-bounded structural basins are developed in the area (Pecsmány, P. *et al.* 2021).

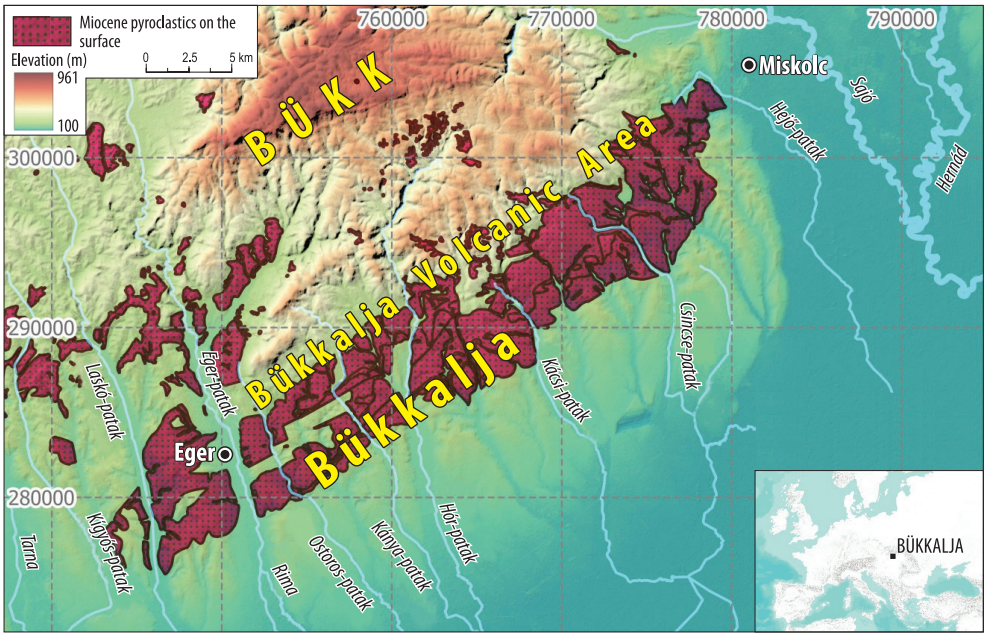

Fig. 1. Topography of the Bükkalja Volcanic Area (BVA) and its vicinities. Inset map shows the location of the Bükkalja. Coordinates are in HD 1972 EOV coordinate system.

The relation between the large-scale topography including the valley and hydrological network of the Bükkalja and the volcanological units was investigated in details by Vágó, J. (2012). However, the link between the topography and the proposed source localities of the ignimbrites (e.g., Szakács, A. *et al.* 1998; Lukács, R. *et al.* 2015; Hencz, M. *et al.* 2021a) that influence the lateral variations in thickness and lithofacies of pyroclastic units has not been investigated in-depth. Therefore, the aim of the present study is to quantify the differences in the statistical distributions of the most obvious topographic parameters of the ignimbrites such as elevation a.s.l., slope, aspect, and topographic openness, in relation to their source localities. In our analysis, special emphasis is given to the welded (i.e., closer to the source localities) or non-welded (i.e., farther to the source localities) character of the ignimbrites.

Geological background

Geomorphology and geology of the Bükkalja Volcanic Area

The Bükkalja is a hilly area between the Bükk Mountains and the Great Hungarian Plain, extending about 60 km in NE-SW and 20–30 km in NW-SE, typically with elevations between 130 and 350 m a.s.l. Its current topography, which is characterized by dips about 5° from the Bükk Mountains. towards the Great Hungarian Plain, is interpreted as a result of pedimentation in three stages, between ~20–14, ~8.0–5.5, 2.0–1.8 Ma (Dobos, A. 2002). During these periods, under typically a semi-arid climate, the slopes of the Bükkalja underwent parallel retreat due to areal water erosion. Today, only several km^2-sized patches of the 2nd and 3rd pedimentation periods have remained, forming an older relict surface between 243–426 m and a younger one between 151–243 m elevation a.s.l. (Vágó, J. and Hegedűs, A. 2011).

The Bükkalja exposes various Paleogene to Quaternary formations: The Oligocene Kiscelli Clay Formation is overlain by Oligocene-Lower Miocene shallow marine beds of variable grain-size belonging to the Eger Formation (Less, Gy. *et al.* 2005). The Paleogene-Lower Miocene sedimentary deposits is in turn overlain by a several 100 m-thick pyroclastic succession emplaced between ~18.2–14.3 Ma from dozens of large explosive eruptions of dominantly high-K rhyolitic magmas (*Figure 2*, Szakács, A. *et al.* 1998; Lukács, R. *et al.* 2018, 2022; Karátson, D. *et al.* 2022). The current surface occurrence of the pyroclastic succession is confined to a ~10 x 40 km region with NE-SW elongation. To keep the nomenclature simple, in this study, the term Bükkalja Volcanic Area (BVA hereafter) is used to refer to the surface occurrence of pyroclastics, which is smaller than the whole area of the Bükkalja. The Miocene pyroclastic succession is overlain by the Pannonian Edelényi Variegated Clay and the Nagyalföldi Formation, which consists of sediments deposited in shallow-sea or by fluvial processes in the gradually filling Pannonian Lake (Less, Gy. *et al.* 2005). The southernmost slopes and larger valleys of the Bükkalja are covered by loess and other Quaternary sandy sediments, which have been redeposited by fluvial processes (Less, Gy. *et al.* 2005).

From a structural geological point of view, the Bükkalja is located between the Mesozoic carbonate mass of the Bükk Mountains, characterized by intensive uplift causing removal of ca. 1 km thick Paleogene-Neogene sedimentary succession during the Pliocene-Pleistocene (between 2 and 3 Ma; Dunkl, I. *et al.* 1994), and the Vatta-Maklár Trench that is interpreted as a "transtensional half-graben" (Petrik, A. 2017) and has been subsiding from the beginning of the Miocene onwards displaying a SW-NE elongation (Petrik, A. 2017). The Bükkalja is also dominated by faults with SW-NE strike, the most significant of which being the Kőkötő Fault, which can be traced on the surface from the SW edge of Eger town to the eastern edge of Bogács village (*Figure 3*, Petrik, A. 2017). Layers of hanging wall blocks displaced along the listric faults are characterized by 2–5° dip and SE dip direction (Petrik, A. 2017).

The pyroclastic succession of the BVA consists of layers from dozens of eruptive events

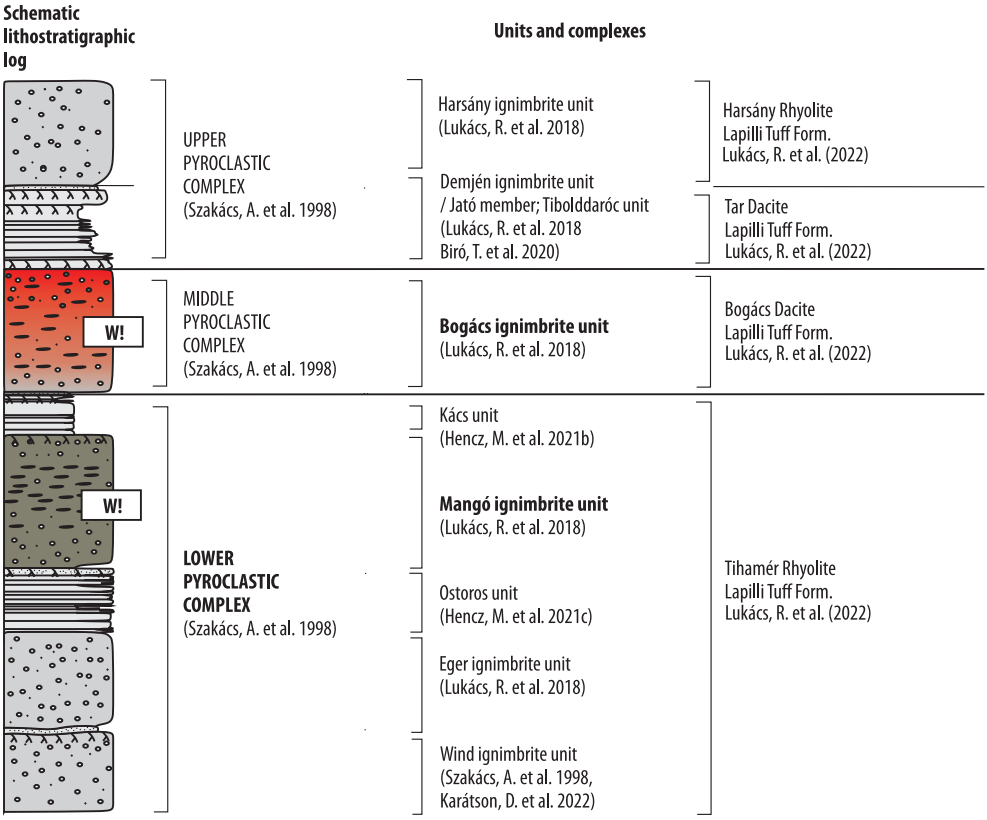

Fig. 2. Generalised lithological column of the BVA after Hencz, M. *et al.* (2021c) and Lukács, R. *et al.* (2022). "W!" marks the ignimbrites which tend to be welded. Thicknesses of stratigraphical units and symbols of components are not to scale.

(see *Figure 2*, Szakács, A. *et al.* 1998; Lukács, R. *et al.* 2018; Biró, T. *et al.* 2020), which, according to the latest stratigraphic classification, belong successively to the Tihamér Rhyolite Lapilli Tuff, the Bogács Dacite Lapilli Tuff, the Tar Dacite Lapilli Tuff and the Harsány Rhyolite Lapilli Tuff Formation (Lukács, R. *et al.* 2022). The pyroclastic deposits include layers of fallout origin, ignimbrites emplaced from pyroclastic density currents, and subordinately epiclastics formed by the resedimentation of the primary pyroclastic material mostly by fluvial processes (Capaccioni, B. *et al.* 1995; Szakács, A. *et al.* 1998; Lukács, R. *et al.* 2007, 2015, 2018; Biró, T. *et al.* 2020; Hencz, M. *et al.* 2021a, b). The pyroclastic layers deposited from distinct eruptive events are generally bounded by palaeosols, suggesting that the BVA was a subaerial region, where pyroclastic material was deposited during eruptive events punctuated by quiescence periods lasting for 10^3–10^5 years, in which soil formation may have occurred (see *Figure 2*, Biró, T. *et al.* 2020). In terms of thickness, the pyroclastic succession is dominated by ignimbrites, of which there are at least 8 in the area, each 20–50 m thick (Lukács, R. *et al.* 2018). Some of these (Wind, Eger, Harsány ignimbrite) are characterized by massive lapilli tuff facies and do not show welding or cementation, while others (Mangó, Bogács, Demjén) show welded lithofacies to some extent (see *Figure 3*).

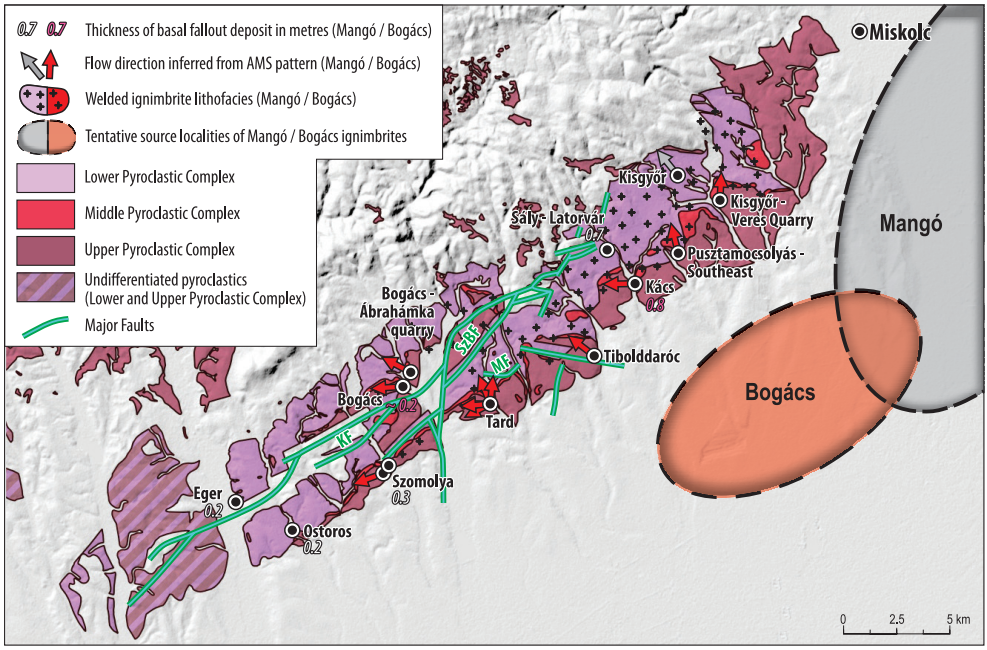

Fig. 3. Volcanological map of the BVA with assumed source localities of the Mangó and Bogács ignimbrites and indicators of source localities. *Sources:* Volcanological map – 1:100 000 Geological map of Hungary (© MBFSz Térképek – https://map.mbfsz.gov.hu/fdt100/) and Lukács, R. *et al.* (2022). Thickness data on the basal fallout deposit of the Mangó and Bogács ignimbrites – Biró, T. *et al.* (2017), Hencz, M. *et al.* (2021a, b). Flow directions based on AMS data – Szakács, A. *et al.* (1998), Cseri, Z. (2017). Source locality of the Mangó ignimbrite – Hencz, M. *et al.* (2021a). Major faults – Petrik, A. *et al.* 2016, Petrik, A. 2017. KF = Kőkötő Fault; SzBF = Szomolya–Bogács Fault; MF = Mangó Fault.

Lithofacies and source localities of the Mangó and Bogács ignimbrites

From a geomorphological point of view, it is very important that the most significant ignimbrites have a welded facies characterized by hard, high-density, erosion-resistant lithology due to compaction after emplacement as a result of >500 °C depositional temperature and significant load stress (e.g., Freundt, A. *et al.* 2000). In general, the thickness of ignimbrites is the most significant at the vicinity of the source vent and in the main valleys, which is manifested by the appearance of welded facies at such settings (Freundt, A. *et al.* 2000). Welded ignimbrite lithofacies can be extremely resistant to erosion, often forming positive/inverted landforms, e.g., mesas, due to millions of years of degradation (Adams, B.A. and Cooper, F.J. 2020; Van Wyk de Vries, B. *et al.* 2022). At the BVA, the Mangó, Bogács and Demjén ignimbrites show welded lithofacies (see *Figure 2*, Lukács, R. *et al.* 2015, 2018; Hencz, M. *et al.* 2021a).

The exact location of the eruption centres that produced the BVA pyroclastic succession is unknown for most units, as the vent areas are no longer detectable in the topography due to several millions of years of basin subsidence and sediment accumulation around the Bükk Mountains (Szakács, A. *et al.* 1998). However, the assumed location of the eruption centre of the Mangó and Bogács ignimbrites, which are characterized by ex-

tensive welded facies, thus, representing hindered erodibility, have been inferred based on multiple proxies: i) flow directions (i.e., direction of lateral shear during emplacement) (Szakács, A. *et al.* 1998), ii) the lateral variations of basal fallout deposit thickness and iii) maximum grain-size of lithics (Hencz, M. *et al.* 2021a).

The Demjén ignimbrite occurs only in the south-western area of the BVA at greater thickness (>20 m) and shows welding, while in the central and eastern areas of the BVA at Bogács and Tibolddaróc (see *Figure 3*) it is less than 10 m thick and fine-grained, discriminated as the 'Jató member' (Biró, T. *et al.* 2020). Consequently, it plays only a very minor role in affecting the topography of the BVA.

The thickening of the basal fallout layer of the Mangó ignimbrite from 0.2 m in the vicinity of Eger to 0.7 m at Sály, and the increase of the maximum lithoclast size, clearly indicate that this ignimbrite was derived from a source area located southeast of the BVA at the southern vicinity of Miskolc (see *Figure 3*, Hencz, M. *et al.* 2021a). The proximity of the eastern region of the BVA to the source locality is also confirmed by the presence of Mangó ignimbrite with a dominantly welded lithofacies in the Kisgyőr area (previously identified as the Kisgyőr Member (Less, Gy. *et al.* 2005; Hencz, M. *et al.* 2021a).

The source locality of the Bogács ignimbrite has been reconstructed from anisotropy of magnetic susceptibility (AMS) directions about 10–15 km south of Tibolddaróc, also supported by a positive Bouguer anomaly (Szakács, A. *et al.* 1998). By considering the thickness variations of the basal fallout layer of the Bogács ignimbrite which ranges from ~0.2 m to 0.8 m from Bogács to Kács (Biró, T. *et al.* 2017; Hencz, M. *et al.* 2021b) the previous localization of the source vent can be slightly shifted and the source region is detected ~10 km from Kisgyőr towards the south (see *Figure 3*).

Thus, both the Mangó and the Bogács ignimbrites are supposed to have been originated from source localities at the southeastern vicinity of the BVA. The aim of the present study is to investigate how the topographic features of the BVA are influenced by the location of the source area of the Mangó and Bogács ignimbrites, with regard to the distribution and lithofacies variations of the two ignimbrites, in particular, welding.

Methods

The analysis of the topography was performed on the SRTM surface model with 1″ (30 m) resolution (NASA 2013) with QGIS 3.18 (QGIS Development Team 2022). A twofold methodology was used to study the topography: 1) The frequency distributions of elevation a.s.l., slope, aspect, positive and negative topographic openness of four sample areas *(Figure 4)* differing in distance from assumed ignimbrite source localities were compared. 2) The topographical features were also investigated along swath profiles.

The four sample areas were delineated by considering the location of assumed source regions of the Mangó and Bogács ignimbrites, the distribution of the Miocene pyroclastics (map.mbfsz.gov.hu/fdt100/; © MBFSz Térképek), the welded or non-welded character of pyroclastics (Pentelényi, L. 2005), the location of the main valleys and the spatial heterogeneity of Bouguer anomaly (map.mbfsz.gov.hu/gravitacios_anomalia/; © MBFSz Térképek). This latter parameter shows the relative depth of the Mesozoic carbonatic basement (*Figure 5*, Petrik, A. 2017), i.e., the amount of Neogene-Quaternary uplift at the BVA. The north-eastern boundary of sample area 1 was set to the north-eastern limit of the LPC (Lower Pyroclastic Complex *sensu* Szakács, A. *et al.* 1998; see *Figure 2*) distribution. Further east, pyroclastic outcrops are rare, so their surface distribution is a matter of some uncertainty (Less, Gy. *et al.* 2005). The boundary between the 1st and the 2nd sample area is defined by the valley of the Kács Stream (Kácsi-patak), west of which the Bouguer anomaly changes, a positive anomaly being observed in the central part of the BVA. The boundary between the 2nd and the 3rd sample

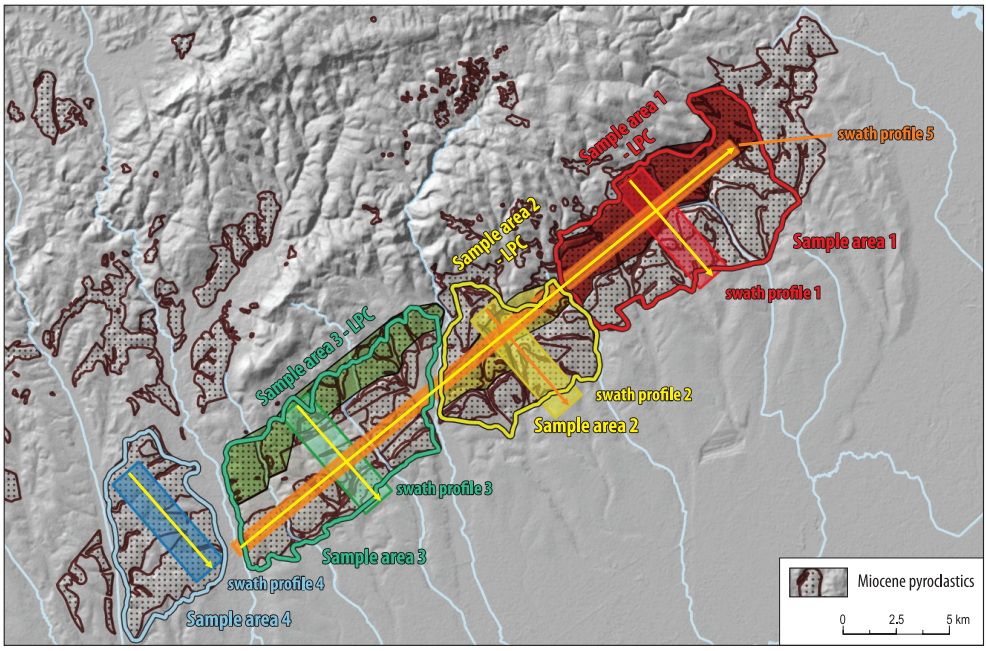

Fig. 4. Sample areas and swath profiles investigated in this study

area is located along the valley of the Hór Stream (Hór-patak). To the west of this, in the area of the 3rd sample area, a small parallel negative Bouguer anomaly is observed NW of the Vatta–Maklár Trench. Furthermore, in the 3rd sample area, the surface distribution of the pyroclastics is split into two 3–5 km wide bands, between which Oligocene and Lower Miocene sedimentary formations are exposed along the so-called Kőkötő Fault (see *Figure 3*, Petrik, A. 2017). The boundary between the 3rd and the 4th sample area is the widest stream valley in the Bükkalja, the Eger Valley. Here, the Bogács ignimbrite is not observed, and the LPC and UPC (Upper Pyroclastic Complex *sensu* Szakács, A. *et al.* 1998; see *Figure 2*) are not clearly separated (Lukács, R. *et al.* 2022; Karátson, D. *et al.* 2022). The 4th sample area is also distinct with respect to the Bouguer anomaly, because it shows a slight positive anomaly like the 2nd sample area.

Slope and aspect maps were generated by the 'Slope' and 'Aspect' tools located in the GDAL Dem Utility of the QGIS. Topographic openness (*sensu* Yokoyama, R. *et al.* 2002) is defined as the mean of 8 zenith (positive topographic openness) or nadir angles (negative topographic openness) within a defined horizontal distance (known as the radial limit) from each cell of a digital elevation model. Positive and negative topographic openness were calculated by the 'Topographic Openness' tool of the QGIS according to Daxter, C. (2020). The radial limit was 1,000 m, the number of sectors was 8 for each analysis. Bin sizes of histograms were specified as follows: 10 m for elevation a.s.l., 2° for slope and 0.1 radian for topographic openness. Circular frequency diagrams also known as 'rose diagrams' were produced from aspect data by using Georose program (Yong Technology 2014). Bin size was set to 10°.

In addition to the analysis of the four sample areas, the LPC areas within the 1st, 2nd and 3rd sample areas were also analysed specifically. The same topographic parameters were analysed, restricted to the surface distribu-

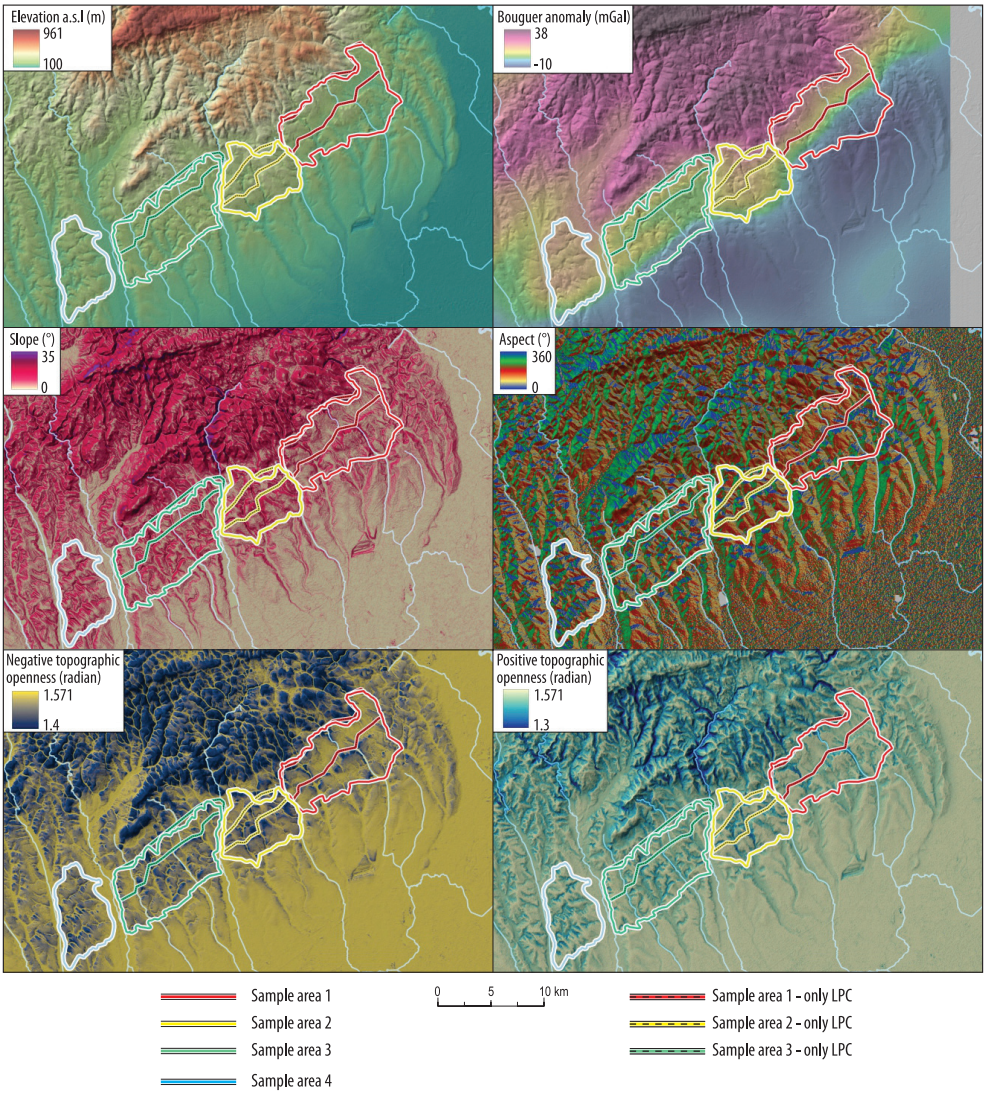

Fig. 5. Elevation a.s.l., Bouguer anomaly, slope, aspect and topographic openness map of the BVA. The Bouguer anomaly map was compiled after the 1:500 000 Bouguer anomaly map of Hungary (© MBFSz Térképek – https://map.mbfsz.gov.hu/gravitacios_anomalia/).

tion of the LPC (see *Figure 3*). In the case of sample area 3 only the northern occurrence of the LPC was considered (which is located towards the north from the Eger–Bogács line), because the southern one is rather influenced by faulting (see *Figure 3*).

Swath profile analysis – a refined version of the classic, line-based cross-section analysis – was also carried out. Swath profiles describe the topography of a greater zone by computing the average, maximum, minimum elevation a.s.l. and the 1st and 3rd quartiles of the

frequency distribution constructed from the elevation values of the pixels of the surface model within a swath with known orientation (for details of the methodology consult Telbisz, T. *et al.* 2011a, 2013). The differences between the curves of the 1st and 3rd quartiles show the variability of the topography. Four of the swaths along which the analysis was carried out had an area of 1.6 x 6 km and the azimuths of their longer sides were generally 140° (clockwise). In addition, a 5th swath profile was also considered covering the LPC from the SW to the NE margin of the BVA (see *Figure 4*). Length and width of this swath profile was 30 000 and 670 m, respectively.

Results

Maps and histograms of elevation a.s.l., slope, topographic openness and aspect

The four sample areas show relevant differences for each of the topographic parameters studied, either the derived maps (see *Figure 5*) or the frequency diagrams (*Figures 6* and *7)*, or the swath profiles are considered *(Figure 8).* The differences between sample areas 1, 2 and 3 are even more pronounced when only the LPC area is considered.

For each sample area, the frequency distribution of elevation a.s.l. resulted in a single-peaked curve. For sample areas 1 and 4, most of the elevation values are between 150 and 250 metres. The average elevation value is slightly higher for sample area 3, where values are typically observed between 175 and 300 m. The highest average elevation is observed at sample area 2 with half of the values above 250 metres. If only the area of LPC is considered, the distributions are different from the previous ones. The values of LPC elevation a.s.l. are the most scattered for sample area 1. Values between 150 and 250 m are most typical, but values between 250 and 350 m are also frequent. Sample area 3, in contrast, shows a distribution characterized by a single peak, with values between 225 and 275 m being the most frequent.

For each sample area, the distribution curve of slope values is generally similar, although slight differences are evident. The most common slope value is below 10 degrees for all sample areas. However, sample area 1 has a higher relative frequency below 6° and a lower relative frequency above 6° than the other 3 sample areas. Most pixels above 10° are observed at sample area 2. The frequency distribution curves for sample areas 3 and 4 are closely similar. If only the LPC areas are considered, the individual sample areas show broadly similar distributions to the previous ones, but the differences between the sample areas are again more remarkable.

As for negative topographic openness, each sample area shows a distribution curve with an individual peak. For sample areas 2, 3 and 4, the most frequent values are closely around 1.5 radians (rad for short hereafter), while for sample area 1 the peak is slightly higher. The curve for sample areas 3 and 4 is also quite similar. In comparison, sample area 1 has more values above 1.5 rad, while sample area 2 has more values below 1.5 rad. Considering only the LPC areas, sample areas 1, 2 and 3 are quite distinct in terms of the distribution of negative topographic openness: although all three sample areas show a single-peaked distribution, the relatively smaller values (<1.5 rad) are observed for sample area 2, while the largest values (>1.5 rad) are observed for sample area 1. Sample area 3 shows a transition between these, with values around 1.5 rad being the most common.

In terms of positive topographic openness, all four sample areas show a substantially similar distribution: the most frequent value is found around 1.55 rad, but there is also a smaller adjacent peak at 1.5 rad beside the main peak. Each sample area differs in terms of the ratio of the two peaks to each other and the significance of the range below 1.45 rad. The minor peak at 1.5 rad is most pronounced for sample area 3 and least significant for sample area 1. The frequency distribution of sample area 2 differs from the other three in that the relative frequency of values below 1.45 rad is notable. The difference be-

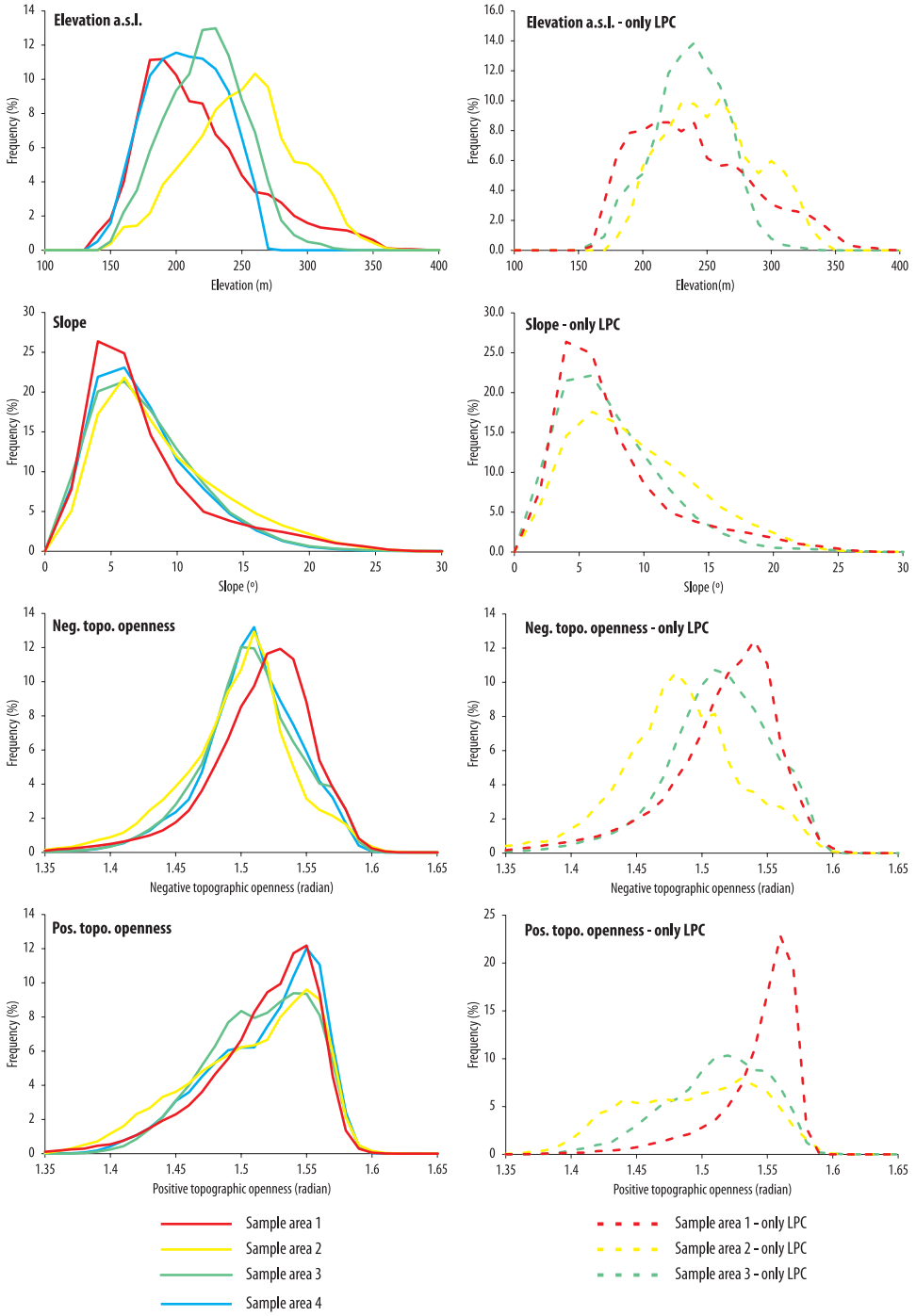

Fig. 6. Frequency distribution of topographic parameters. Note, that the dashed curves refer to sample areas restricted to the LPC surfaces only.

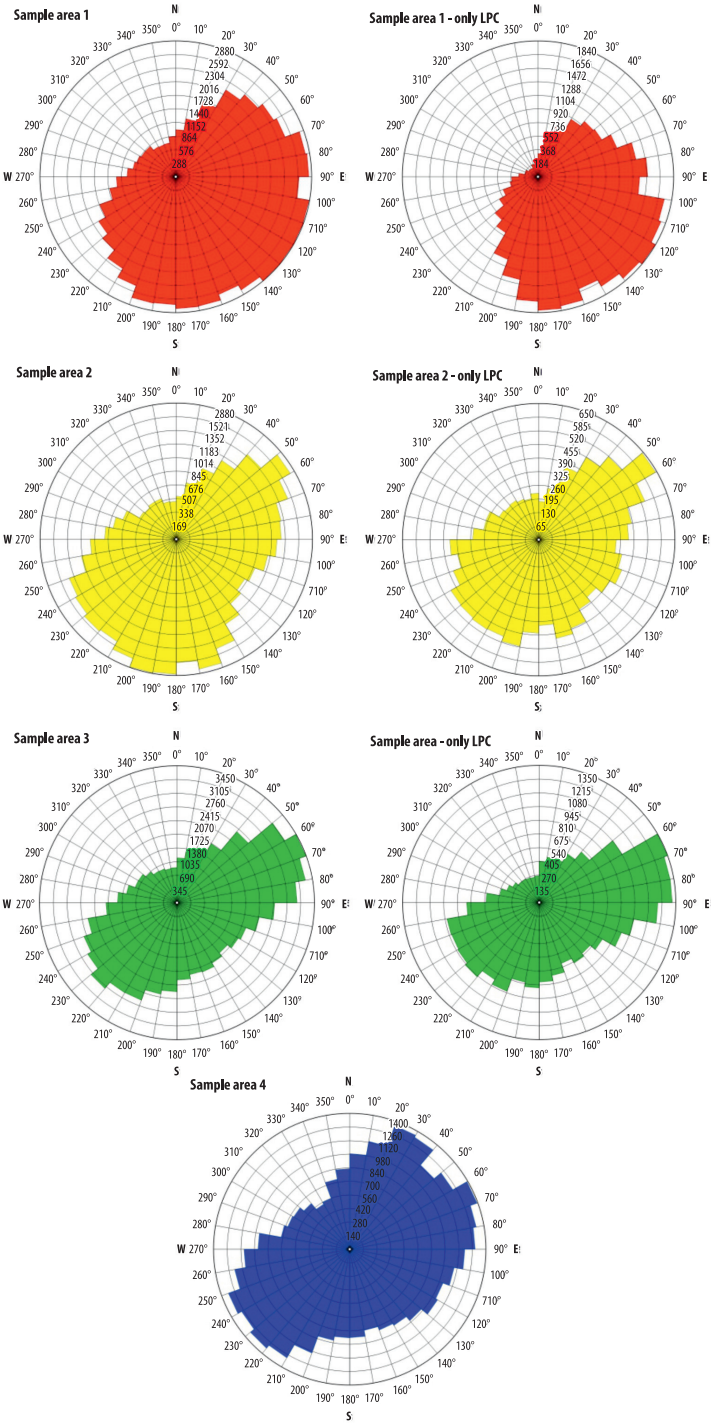

Fig. 7. Rose diagrams showing aspect distribution of the sample areas

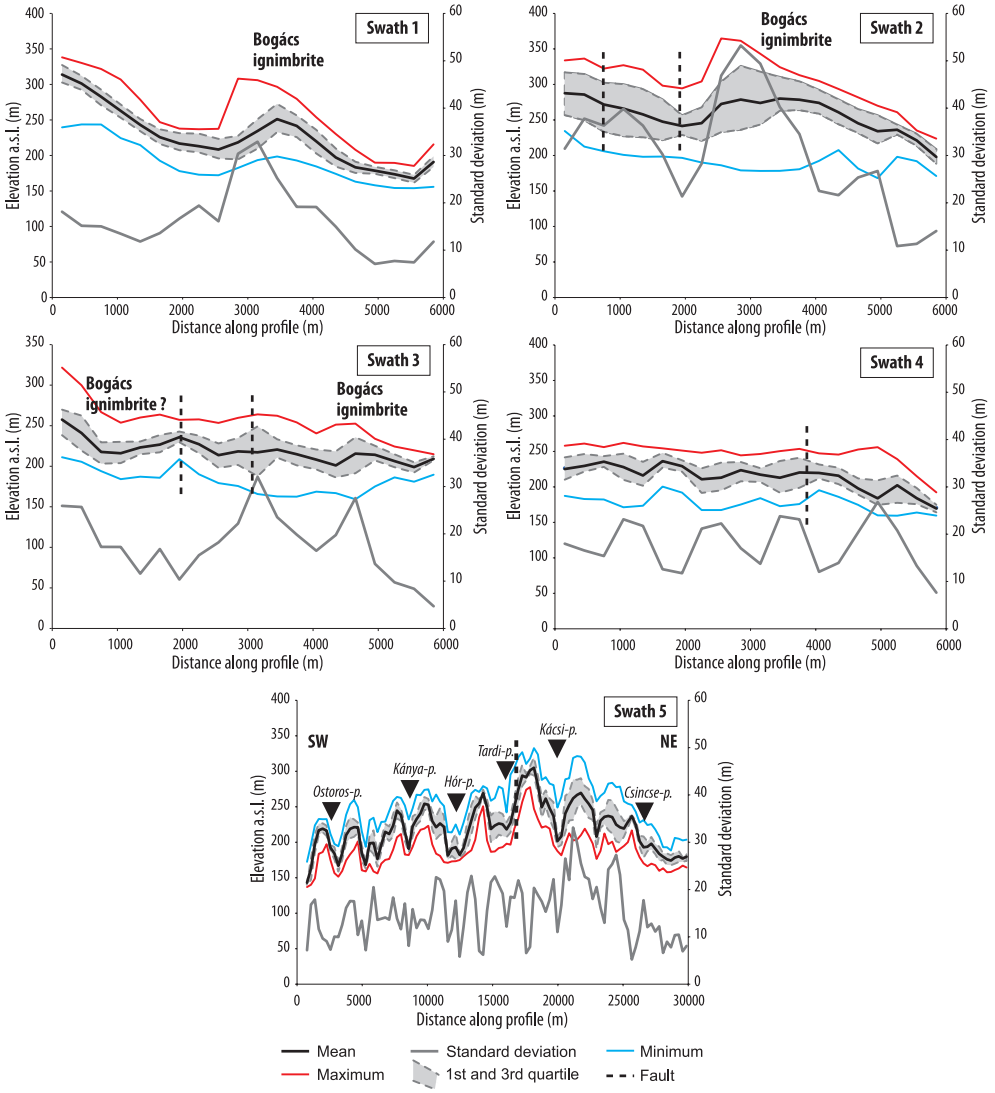

Fig. 8. Swath profiles investigated in this study. Faults are adapted from Petrik, A. (2017).

tween sample areas 1, 2 and 3 is most evident in the positive topographic openness values obtained for the LPC areas. For sample area 1, a significant peak is observed at 1.55 rad. In contrast, sample area 2 shows a flat tail, with values between 1.45 rad and 1.55 rad being virtually uniformly frequent. Sample area 3 shows a transition between the two.

Based on aspect values, sample area 1 is considered to be unimodal, dominated by aspect values between 70° and 200°. The relative frequency of pixels facing to NW is much lower here. In contrast, pixels facing NE and SW are the most prominent at the other three sample areas. It is important to note that sample area 2 differs slightly from

this group, as S-facing pixels are also frequent in addition to NE and SW directions. Similarly, sample area 4 has a significant contribution of E-facing pixels in addition to the dominant NE and SW directions.

Topographic swath profile analysis

The different character of the topography of the study areas is also evident by considering the swath profiles (see *Figure 8*). The most important information that can be derived from the swath profiles is the different relative degree of dissection of the LPC surfaces in the northern and north-western forefronts of the Bogács ignimbrite occurrences along swath 1, 2 and 3. The degree of the dissection is indicated by the difference between the Q1 and Q3 curves on the one hand, and the standard deviation along the profile on the other. It is obvious that the LPC shows the smallest topographic variability along swath 1, even though this is the steepest slope. The highest variability is observed for swath 2.

Furthermore, it is also apparent that between swath 1 to 3 the relative height of the Bogács ignimbrite with respect to the LPC surface gradually decreases from ~40 m to less than 20 m. Swath profile 5 shows the topographical change of the LPC from the SW towards the NE edge of the BVA. It shows, that although the standard deviation of elevation a.s.l. is higher at the NE part of the BVA, the valleys are generally deeper at its SW part.

Discussion

Foothill geomorphology principally affected by ignimbrite lithofacies

Present results show that the elevation a.s.l., slope, aspect and topographical openness of sample areas 1 and 3, 4 show a marked difference: the dominant features of the topography of sample area 1 are the tilted slabs facing S, SE and are characterized by relatively minor fluvial dissection, while the other sample areas show a topography significantly dissected by fluvial erosion.

The frequency distribution of elevation a.s.l. at sample area 1 shows an asymmetric distribution, which is different from the other three sample areas. The distribution of elevation a.s.l. at the other 3 sample areas shows a symmetrical distribution. This type of frequency distribution is typical of the relief dissected by fluvial erosion (e.g., Telbisz, T. *et al.* 2011b). The most frequent value in sample area 1 is less than 5° in the frequency distribution of the slope, which is especially evident when considering only the LPC surface. It is worth noting that the predominant components of the valley network here are the steep-sided valleys with a NW-SE orientation, which separate the tilted slabs protected by the Mangó ignimbrite. Only in the NW vicinity of the Bogács ignimbrite surficial occurrence there are minor valleys inclined or perpendicular to this direction. Thus, the lack of well-evolved, multidirectional valley network results in the lack of abundant higher slope values compared to the other sample areas. Further on, the dominance of the tilted welded ignimbrite slabs is also reflected in the aspect distribution. The tilted slab formed by the Mangó ignimbrite is still more or less present at sample area 2, but is much more dissected due to the more intense incision resulting in the higher proportion of slope values greater than 10°. For sample areas 3 and 4, the south and southeast sloping slabs are absent and are replaced by erosional valleys with a multidirectional network having a predominant influence on aspect values, too. The difference of sample area 1 on the frequency diagram of topographic openness from the other sample areas is also due to this reason. In areas where the degree of dissection is limited, the frequency distribution of topographic openness will be dominated by a pronounced peak. On the other hand, where the topography is composed of valleys and ridges, the frequency distribution of topographic openness becomes two-peaked, i.e., the peak at lower values of negative topographic openness is typical of ridges, while the peak at relatively higher values is typical of valley bottoms (see

Figure 5 in Yokoyama, R. *et al.* 2002). In fact, sample area 1 has higher values than the other three sample areas both regarding negative and positive topographic openness, indicating that there is a relatively lower degree of erosional dissection here.

By taking into consideration the relative location of various sample areas from the source localities of the Mangó and Bogács ignimbrites, a pronounced difference between sample area 1, which is the closest to the vent area (within 10–20 km), and sample areas 3 and 4, which are further away by 30–40 km, is evident. The dominance of tilted slabs of welded ignimbrites in the topography around Kisgyőr and their absence in the SW part of the BVA has already been recognised by Pentelényi, L. (2005), Vágó, J. (2012), and Vágó, J. and Hegedűs, A. (2011). It has also become evident that the occurrences of the Bogács ignimbrite are characterized by the highest relative relief in the BVA (>100 m/km^2), and that the surface of the welded lithofacies of the Mangó ignimbrite (Kisgyőr Ignimbrite member *sensu* Pentelényi, L. 2005) typically exhibits low slope values as a consequence of the tilted plateau morphology (Vágó, J. and Hegedűs, A. 2011). However, a systematic study of the topographic features of the BVA along its NE-SW extension, taking into account that the ignimbrites of the NE areas (Mangó and Bogács), which are closer to the source localities tend to be welded, has not been carried out so far.

The stratigraphic succession of pyroclastic-dominated volcanic fields frequently contains units of extremely variable erodibility (e.g., friable vs. densely welded ignimbrites), which has a crucial influence on the extent, shape and temporal variability of both small- and large-scale landforms i.e., from river terraces to several 100 km^2-large ignimbrite plateaus (Yokoyama, S. 1999; Karátson, D. *et al.* 2009; Székely, B. *et al.* 2014; Adams, B.A. and Cooper, F.J. 2020). Present results show that the topography of the BVA is fundamentally controlled by spatial variations of the lithofacies of the Mangó and Bogács ignimbrites related to the distance from their source area. Both the Mangó and Bogács ignimbrites have their highest relative thickness, often exceeding 30 m, in sample area 1, and in the same area, both ignimbrites display a typical welded lithofacies characterized by fiamme structures and low porosity (Pentelényi, L. 2005, Hencz, M. *et al.* 2021a, b). At the western part of the BVA associated with sample areas 3 and 4 the Mangó ignimbrite is still more than 20 m thick, however, it shows non-welded, rather friable lithofacies (e.g., at the eastern vicinity of Eger; Biró, T. *et al.* 2017; Hencz, M. *et al.* 2021a). Towards SW, the Bogács ignimbrite is thickening gradually and even disappears approximately in the central part of sample area 3, east of Ostoros (see *Figure 3*). Consequently, the topography of sample area 1, which is relatively closer to the source region, is characterised by slabs tilted south-east by up to 10° dip angle, and composed of welded lithofacies of the Mangó and Bogács ignimbrites. This is particularly evident in the case of the LPC surface, which is dominated here by the welded Mangó ignimbrite, which has preserved its less dissected, slab-like appearance despite the fact that the topographic gradient, i.e., the degree of tilting from the original presumably near-horizontal bedding (Biró, T. *et al.* 2020), is the most significant here.

Although the distinct topography of the SW and NE parts of the BVA can be explained by the lateral facies variations of the Bogács and Mangó ignimbrites, the results suggest that the topography of the BVA is also influenced by the total amount and direction of vertical movements.

The effect of vertical movements on fluvial dissection at the BVA

The degree of dissection does not vary unidirectionally between sample areas 1 and 4. Instead, it was observed that sample area 2 has a greater relative depth of valleys than sample areas 3 and 4, despite the fact that here the Mangó ignimbrite still has a welded facies (Pentelényi, L. 2005). Sample area 2 has the highest average

elevation a.s.l. and shows a positive Bouguer anomaly compared to the other sample areas (see *Figures 6* and *8*). Both the higher average elevation a.s.l. and the positive Bouguer anomaly suggest a more intense uplift here than at all other sample areas. As a consequence, valley incision is also most intense here and both the LPC outcrop and the Bogács ignimbrite are the most intensively dissected here. This is probably also in relation to the fact that this is the region of the BVA where the largest number of fairy chimneys (tent rocks or beehive rocks) carved by water erosion from unconsolidated ignimbrite occur (Borsos, B. 1991). The formation of the fairy chimneys in this region was probably facilitated by the more intense uplift and related effective fluvial incision.

Conclusions

The frequency distributions of elevation a.s.l., slope, aspect as well as positive and negative topographic openness were investigated at the Bükkalja Volcanic Area (BVA) using a 30 m resolution SRTM-based digital terrain model at four sample areas located at different relative distances from the assumed source localities of the ignimbrites showing welded facies. At these sample areas we also investigated the degree of dissection along swath profiles. Based on the results obtained, the following conclusions can be drawn:

All morphometric parameters investigated show a remarkable difference between sample areas located closer and further away from the source localities. The topography of the sample area closest to the source localities (i.e., the eastern part of the BVA) is dominated by slabs of moderately dissected welded ignimbrites, gently dipping towards SE. This topography appears as an asymmetric curve in the frequency distribution of elevation a.s.l., showing a slight overplus for the higher values, increasing the frequency of less than 5° slope values and SE-facing pixels, and resulting in a distribution of single-peaked positive and negative topographic openness with higher frequencies for larger values than in case of the other sample areas. The topography of the sample areas farther away from the source localities (i.e., in the western part of the BVA) is dominated by erosional valleys and ridges, resulting in a narrower typical elevation range, a higher proportion of pixels with greater than 5° slope compared to sample area 1, and higher frequencies of NE and SW exposures. At these sample areas, the more significant incision has resulted in more frequent pixels with positive topographic openness less than 1.5 radians.

The increasing dissection of the BVA from NE towards SW is principally controlled by the change in the lithofacies of the Mangó and Bogács ignimbrites, via the dominance of welded facies within sample areas 1 and 2, the decrease in thickness, and the disappearance of welded lithofacies in the SW direction.

In addition to the location of the ignimbrite source regions, the degree of dissection at the BVA is also influenced by the relative amount of vertical uplift, as the most dissected sample area coincides with the region with the largest positive Bouguer anomaly and average elevation a.s.l.

The overall implication of the present study is that the degree of dissection of millions of years old ignimbrite fields is fundamentally determined by the thickness and lithofacies (welded vs non-welded) of the ignimbrites that may show a large lateral variability. Since higher thicknesses and temperatures, and consequently welded facies, are more common closer to the source vent, the erosion pattern can be used to draw conclusions on the spatial aspects of the most intense ignimbrite aggradation, i.e., the location and vicinity of eruption centres in deeply eroded ignimbrite fields.

Acknowledgement: Present research was supported by the ÚNKP-21-4 New National Excellence Program of the Ministry for Innovation and Technology from the source of the National Research, Development and Innovation Fund (ÚNKP-21-4-II-ELTE-382; ÚNKP-21-4-I-ELTE-63) and by the Hungarian National Fund (NKFIH-OTKA K131894). We thank Károly Németh and Zoltán Pécskay for fruitful discussions on the landforms of ignimbrite-dominated landscapes.

REFERENCES

Adams, B.A. and Cooper, F.J. 2020. *The importance of ignimbrite armour on mountain range evolution.* American Geophysical Union. Fall Meeting Abstracts, EP031-0019. Available at https://ui.adsabs.harvard.edu/abs/2020AGUFMEP0310019A/abstract

Biró, T., Kovács, I.J., Karátson, D., Stalder, R., Király, E., Falus, Gy., Fancsik, T. and Sándorné, J.K. 2017. Evidence for post-depositional diffusional loss of hydrogen in quartz phenocryst fragments within ignimbrites. *American Mineralogist: Journal of Earth and Planetary Materials* 102. (6): 1187–1201.

Biró, T., Hencz, M., Németh, K., Karátson, D., Márton, E., Szakács, A., Bradák, B., Szalai, Z., Pécskay, Z. and Kovács, I.J. 2020. A Miocene phreatoplinian eruption in the north-eastern Pannonian Basin, Hungary: the jató member. *Journal of Volcanology and Geothermal Research* 401. Doi:10.1016/j.jvolgeores.2020.106973

Borsos, B. 1991. A bükkaljai kaptárkövek földtani és felszínalaktani vizsgálata (Geological and geomorphological investigation of the beehive-rocks of the Bükkalja). *Földrajzi Közlemények* 115. (3–4): 121–137.

Capaccioni, B., Coradossi, N., Harangi, R., Harangi, Sz., Karátson, D., Sarocchi, D. and Valentini, L. 1995. Early Miocene pyroclastic rocks of the Bükkalja Ignimbrite Field (North Hungary) – A preliminary stratigraphic report. *Acta Vulcanologica* 7. (2): 119–124.

Crowe, B.M., Linn, G.W., Heiken, G. and Bevier, M.L. 1978. *Stratigraphy of the Bandelier Tuff in the Pajarito Plateau. Applications to waste management.* Report no. LA-7225-MS. Los Alamos, New Mexico, USA. Los Alamos Scientific Laboratory. Doi:10.2172/6870764.

Cseri, Z. 2017. *A bükkaljai ignimbritek mágneses szuszceptibilitás anizotrópiájának jellemzői.* (Features of anisotropy of magnetic susceptibility of ignimbrites at the Bükkalja). MSc Thesis, Budapest, ELTE Faculty of Science, Department of Physical Geography.

Daxter, C. 2020. *Topographic Openness Maps and Red Relief Image Maps in QGIS.* Innsbruck, University of Innsbruck, Institute of Geology.

Dobos, A. 2002. A Bükkalja II. felszínalaktani leírás. (The Bükkalja II. geomorphological description). In *A Bükki Nemzeti Park.* Ed.: Baráz, Cs., Eger, Bükki Nemzeti Park Igazgatóság, 217–228.

Dunkl, I., Árkai, P., Balogh, K., Csontos, L. and Nagy, G. 1994. A hőtörténet modellezése fission track adatok felhasználásával – a Bükk hegység kiemelkedéstörténete (Thermal modelling based on apatite fission track dating – the uplift history of the Bükk Mountains). *Földtani Közlöny* 124. (1): 1–24.

Freundt, A., Wilson, C.J.N. and Carey, S.N. 2000. Ignimbrites and block-and-ash flow deposits. In *Encyclopaedia of Volcanoes*. 1st edition. Ed.: Sigurdsson, H., New York, Academic Press, 581–599.

Hencz, M., Biró, T., Cseri, Z., Karátson, D., Márton, E., Németh, K., Szakács, A., Pécskay, Z. and Kovács, I.J. 2021a. A Lower Miocene pyroclastic-fall deposit from the Bükk Foreland Volcanic Area, Northern Hungary – clues for an eastward-located source. *Geologica Carpathica* 72. (1): 26–47.

Hencz, M., Biró, T., Cseri, Z., Németh, K., Szakács, A., Márton, E., Pécskay, Z. and Karátson, D. 2021b. Egy összetett kitörési eseménysorozat nyomai a Bükkalján (Észak-Magyarország): a Kács Egység (Signs of complex eruption events at the Bükk Foreland [Northern Hungary]: the Kács Member). In *22nd Mining, Metallurgy and Geology Conference. Abstracts.* Cluj, Hungarian Technical Scientific Society of Transylvania. 71–75.

Hencz, M., Biró, T., Kovács, I.J., Stalder, R., Németh, K., Szakács, A., Pálos, Z., Pécskay, Z. and Karátson, D. 2021c. Uniform "water" content in quartz phenocrysts from silicic pyroclastic fallout deposits – implications on pre-eruptive conditions. *European Joural of Mineralogy* 33. (5): 571–589.

Hevesi, A. 2002. Fejlődéstörténet II. Felszínfejlődés (Surface evolution II. Surface development). In *A Bükki Nemzeti Park.* Ed.: Baráz, Cs., Eger, Bükki Nemzeti Park Igazgatóság, 83–108.

Karátson, D., Telbisz, T., Székely, B. and Wörner, G. 2009. *Style, rate and pattern of erosion on stratovolcanoes and ignimbrite surfaces in the Central Andes.* EGU General Assembly Conference. Geophysical Research Abstracts, Vol. 11. 10547-1.

Karátson, D., Biró, T., Portnyagin, M., Kiss, B., Jean-Louis, P., Cseri, Z., Hencz, M., Németh, K., Lahitte, P., Márton, E., Kordos, L., Józsa, S., Hably, L., Müller, S. and Szarvas, I. 2022. Large-magnitude (VEI ≥ 7) 'wet' explosive silicic eruption preserved a Lower Miocene habitat at the Ipolytarnóc Fossil Site, North Hungary. *Scientific Reports* 12. Article number 9743.

Leonard, G.S., Begg, J.G. and Wilson, C.J.N. 2010. *Geology of the Rotorua Area. Institute of Geological and Nuclear Sciences 1:250 000 geological map 5.* Lower Hutt, New Zealand, GNS Science.

Less, Gy., Kovács, S., Pelikán, P., Pentelényi, L. and Sásdi, L. 2005. *Geology of the Bükk Mountains. Explanatory book to the geological map of the Bükk Mountains (1:50 000).* Budapest, Hungarian Institute of Geology and Geophysics.

Lukács, R., Harangi, Sz., Ntaflos, T., Koller, F. and Pécskay, Z. 2007. A Bükalján megjelenő felső riolittufaszint vizsgálati eredményei: a harsányi ignimbrit egység. (The characteristics of the Upper Rhyolite Tuff Horizon in the Bükkalja volcanic field: The Harsány ignimbrite unit). *Földtani Közlöny* 137. (4): 487–514.

Lukács, R., Harangi, Sz., Bachmann, O., Guillong, M., Danisik, M., Buret, Y, von Quadt, A., Dunkl, I., Fodor, L., Sliwinski, J., Soós, I. and Szepesi, J. 2015. Zircon geochronology and geochemistry to

constrain the youngest eruption events and magma evolution of the Mid-Miocene ignimbrite flare-up in the Pannonian Basin, eastern-central Europe. *Contributions to Mineralogy and Petrology* 170. Article number 52.

Lukács, R., Harangi, Sz., Guillong, M., Bachmann, O., Fodor, L., Buret, Y., Dunkl, I., Sliwinski, J., von Quadt, A., Peytcheva, I. and Zimmerer, M. 2018. Early to Mid-Miocene syn-extensional massive silicic volcanism in the Pannonian Basin (East-Central Europe): Eruption chronology, correlation potential and geodynamic implications. *Earth Science Reviews* 179. 1–19.

Lukács, R., Harangi, Sz., Gál, P., Szepesi, J., Di Capua, A. and Fodor, L. 2022. Formal definition and description of lithostratigraphic units related to the Miocene silicic pyroclastic rocks outcropping in Northern Hungary: A revision. *Geologica Carpathica* 73. 137–158.

NASA 2013. *Shuttle Radar Topography Mission (SRTM) Global*. Distributed by OpenTopography.

Pecsmány, P. and Vágó, J. 2020. A mélyszerkezet és a domborzat közötti kapcsolat a Bükkalja területén (Relationship between geological structure elements and topography in the Bükkalja). *Műszaki Földtudományi Közlemények* 89. (1): 29–34.

Pecsmány, P., Hegedűs, A. and Vágó, J. 2021. DEM based morphotectonical analysis of the Kisgyőr Basin (Bükk Mountains, Hungary). *Acta Montanistica Slovaca* 26. (2): 364–374.

Pecsmány, P. 2021. A Bükkalja völgyhálózatának rendűség szerinti iránystatisztikai vizsgálata (Quantitative analysis of drainage network direction in the Bükkalja). *Multidisciplináris Tudományok* 11. (2): 9–16.

Pentelényi, L. 2005. A bükkaljai miocén piroklasztikum összlet (The Miocene pyroclastic assemblage of Bükkalja). In *A Bükk hegység földtana. Magyarázó a Bükk-hegység földtani térképéhez (1:50 000).* Ed.: Pelikán, P., Budapest, MÁFI, 110–125.

Petrik, A., Beke, B., Fodor, L. and Lukács, R. 2016. Cenozoic structural evolution of the southwestern Bükk Mountains and the southern part of the Darnó Deformation Belt (NE Hungary). *Geologica Carpathica* 67. (1): 82–104.

Petrik, A. 2017. *A Bükk déli előterének kainozoós szerkezetalakulása* (Cenozoic structural evolution of the Southern Bükk foreland). PhD Thesis, Budapest, ELTE Faculty of Science.

QGIS Development Team 2022. *QGIS Geographic Information System*. Open Source Geospatial Foundation. URL http://qgis.org

Szakács, A., Márton, E., Póka, T., Zelenka, T., Pécskay, Z. and Seghedi, I. 1998. Miocene acidic explosive volcanism in the Bükk Foreland, Hungary: Identifying eruptive sequences and searching for source locations. *Acta Geologica Hungarica* 41. (4): 413–435.

Székely, B., Koma, Zs., Karátson, D., Dorninger, P., Wörner, G., Brandmeier, M. and Nothegger, C. 2014. Automated recognition of quasi-planar ignimbrite sheets as paleosurfaces via robust segmentation of digital elevation models: an example from the Central Andes. *Earth Surface Processes and Landforms* 39. (10): 1386–1399.

Telbisz, T., Kovács, G. and Székely, B. 2011a. Sávszelvények készítése és elemzése (Creating swath profiles and swath analysis). In *Lehetőségek a Domborzatmodellezésben. A HunDEM 2011 Kerekasztal és Konferencia Közleményei*. Ed.: Hegedűs, A., Miskolc, Miskolci Egyetem Földrajz Intézet, 1–8.

Telbisz, T., Mari, L. and Szabó, L, 2011b. Geomorphological characteristics of the Italian side of Canin Mountains (Julian Alps) using digital terrain analysis and field observations. *Acta Carsologica* 40. 255–266.

Telbisz, T., Kovács, G., Székely, B. and Szabó, J. 2013. Topographic swath profile analysis: a generalization and sensitivity evaluation of a digital terrain analysis tool. *Zeitschrift für Geomorphologie* 57. (1): 485–513.

Van Wyk de Vries, B., Karátson, D., Gouard, C., Németh, K., Rapprich, V. and Aydar, E. 2022. Inverted volcanic relief: Its importance in illustrating geological change and its geoheritage potential. *International Journal of Geoheritage and Parks* 10. (1): 47–83.

Vágó, J. and Hegedűs, A. 2011. DEM based examination of pediment levels: a case study in Bükkalja, Hungary. *Hungarian Geographical Bulletin* 60. (1): 25–44.

Vágó, J. 2012. *A kőzetminőség szerepe a Bükkalja völgy- és vízhálózatának kialakulásában* (The effects of rock quality on the valley and drainage network of Bükkalja). PhD Thesis. Miskolc, University of Miskolc.

Yokoyama, S. 1999. Rapid formation of river terraces in non-welded ignimbrite along the Hishida River, Kyushu, Japan. *Geomorphology* 30. (3): 291–304.

Yokoyama, R., Shirasawa, M. and Pike, R.J. 2002. Visualizing topography by openness: a new application of image processing to digital elevation models. *Photogrammetric Engineering and Remote Sensing* 68. (3): 257–266.

Yong Technology 2014. *GeoRose*. Edmonton, CAN, Yong Technology Inc. Available at http://www.yongtechnology.com/download/georose

Web sources:

1:100 000 Geological map of Hungary. Available at https://map.mbfsz.gov.hu/fdt100/

1:500 000 Bouguer anomaly map of Hungary. Available at https://map.mbfsz.gov.hu/gravitacios_anomalia/